Exploring the Optical and Electronic Properties of Xylindein, a Fungus-Derived Pigment, as a Sustainable Organic Semiconductor

Alexander Quinn
Oregon State University
Department of Physics
5 June 2018

Advisor: Oksana Ostroverkhova
Oregon State University
Department of Physics

Abstract

Xylindein is an organic pigment derived from Chlorociboria aeruginascens and C. aeruginosa fungi that has shown promise as an organic semiconductor. Preliminary estimates of charge carrier mobilities (CCMs) on the order of 0.1 $cm^2/V \times s$ were calculated from early tests on xylindein thin films, and photocurrents were also observed under laser stimulation. As part of the ongoing effort to characterize xylindein and improve its quality as a possible semiconductor, a broad set of experiments were performed testing the optical and electronic properties of xylindein in solutions and bulk films, and attempts were made, using techniques like solvent vapor annealing, to improve the electronic quality of xylindein thin films (as measured by CCM). In addition, the electronic properties of xylindein and some of its isomers were calculated using Gaussian 09. The details of these experiments and their results are outlined in this report, with comparisons made between the observed characteristics of xylindein and those of other organic semiconductors.

Xylindein absorbs strongly in the visible range, with a peak molar absorptivity near 8600 $1/M \times cm$, but fluoresces very little compared to other organic semiconductors, indicating some strong mechanism for non-radiative decay in both dissoved and bulk xylindein. Xylindein shows strong signs of intermolecular hydrogen bonding through both a 30-60 nm red shift in the absorption spectrum in protic solvents as well as a tendancy to start showing bulk properties in spectroscopic data at a lower range of solution concentrations than other organic semiconductors. The high preliminary charge carrier mobilities observed were not successfully replicated, but efforts to improve thin film quality were unsuccessful or even counterproductive. Computational results for enthalpy of formation ΔH_f show a difference of less than 0.1 kcal/mol between xylindein and one of its isomers, suggest that xylindein could potentially spontaneously self-isomerize. The isomers of xylindein were also calculated to have vastly different HOMO-LUMO gaps, with sizes ranging from 1.70 to 2.24 eV, than xylindein itself.

Contents

List of Figures

1 Introduction

In recent years, interest has grown in the field of organic electronics. As the need for renewable, environmentally-friendly technologies is increasingly recognized, the push has become stronger to develop alternatives to traditional electronic devices based on inorganic semiconductors like silicon. Already, organic materials have seen widespread commercial application in LED screens and displays, and further applications are being intensely studied [1]. Of particular note are organic transistors [2,3,4] and organic photovoltaics (OPVs) [5, 6, 7], though a host of other applications have been explored.

The material characterized in this research is xylindein (Figure 1), a blue-green pigment produced by the wood-staining fungi *Chlorociboria aeruginascens* and *C. aeruginosa* [8]. Though the structure of xylindein has been known since 1965, its has not been successfully synthesized in the laboratory [9]. All characterization performed on xylindein has been done on samples derived from natural sources.

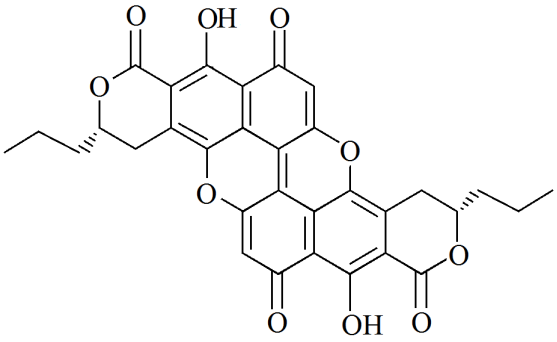

Figure 1: Xylindein - An organic pigment derived from *C. aeruginascens* fungus

The goal of this research is to assess the usefulness of xylindein as an organic semiconductor by characterizing its electronic and optical properties (including bulk charge carrier mobility, absorptivity, and electronic energy levels) and material stability as a single molecule and as a thin film by assessing these characteristics through a mixture of experimental and computational work and by comparing these characteristics to those of benchmark organic semiconductors (such as ADT-TES-F and Pn-TIPS) and conventional inorganic semiconductors.

1.1 Organic Semiconductors

In general, organic materials are insulators. Organic crystals are held together mainly by dispersion forces, so coupling between molecules is weak, and charge carriers are localized. Organic semiconductors, organic materials capable of supporting substantial electric currents, are an exception to this trend, due largely to other forms of intermolecular interaction, such as π-stacking and hydrogen bonding. Given xylindein's extensive system of π-bonded carbons and its pair of oxygen-hydrogen bonds, it appears to be a strong candidate for use as an organic semiconductor.

1.1.1 Pi-Stacking

Most molecules used as organic semiconductors have a large network of carbon-carbon double bonds (as can be seen for xylindein in Figure 1). When two C-C double bonds are adjacent (i.e. separated only by a single bond), they form a conjugated π-bond, meaning the electrons in each individual bond become delocalized. These delocalized electrons form "ribbons" of charge extending along the entire conjugated area.

Because π-bonds produce regions of high and low electron density, they can promote intermolecular attraction between π-conjugated molecules. This can result in π-stacking, an ordered structural arrangement seen in conjugated materials. Materials that exhibit π-stacking often have high charge carrier mobilities.

1.1.2 Hydrogen Bonding

Hydrogen bonding is coupling between molecular side-groups resulting from interaction between a positively polarized hydrogen on one group and an electronegative atom (O, N, F, etc.) on another group. Coupling can be between groups on different molecules (intermolecular hydrogen bonding) or different groups on the same molecule (intramolecular hydrogen bonding). The presence of hydrogen bonding has been correlated with improved charge carrier mobility and device performance [4].

1.1.3 Molar Absorptivity

As light travels through a solution, its intensity is attenuated in a way described by the Beer-Lambert law

$$A \equiv \log_{10} \frac{I_0}{I} = \epsilon l c \tag{1}$$

where I_0 and I are the initial and final intensities, respectively, A is absorption, l is distance traveled through the solution, c is solution concentration, and ϵ is molar absorptivity. Absorptivity generally varies with applied wavelength, and molar absorptivity is often reported as the maximum value observed along with its respective wavelength. Compared to other organic molecules, pigments have very high molar absorptivities in the visible range compared to other organic molecules, and this property is highly desirable for OPVs, as materials that do not absorb light in the visible spectrum will not be able to convert the energy from sunlight into electronic energy efficiently.

Absorption can occur due to electron excitation (the transition of an electron from the ground state to an excited state) or the excitation of molecular vibrational modes. Electron excitation is desirable, as it allows electrons and holes to be separated and current to be generated under an applied electric field. Molecular vibration is usually induced by light in the infrared range, meaning absorption due to it will not directly show up in spectroscopy in the visual range. However, vibrational modes can couple with electronic transitions, producing higher-energy transitions that show up in spectroscopy as vibronic peaks.

Differences in absorption spectra can be expected between single molecules in solution and solid crystals/amorphous films. Molecular coupling (for example, through hydrogen bonding or π-bonding) lowers the energy levels of excited states, resulting in a red-shifting of the single-molecule spectrum.

1.1.4 Photoluminescence

Photoluminescence (PL) is the emission of light caused by the electronic transition from an excited state induced by the absorption of a photon to the ground state. PL takes place spontaneously, and any excited state will eventually decay and release a photon unless its energy is dissipated by some other mechanism, like direct conversion to thermal energy.

1.2 Organic Electronics

1.2.1 Photovoltaics

Organic photovoltaics (OPVs) convert light energy to useful electric current. Most OPVs have two components – an electron donor and an electron acceptor. Stimulation of one component by light can excite electrons from their ground state into their excited state, creating an exciton (an bound electron-hole pair). If this exciton is able to drift to the boundary between an electron donor region and an electron acceptor region before collapsing, it will split into an electron and a hole. In the presence of an electric field, these

charge carriers travel in opposite directions, producing a net current [5].

In practice, most OPVs consist of an organic film on a substrate between two electrodes. The electrodes are typically made of different metals, since a difference between the electrode work functions will generate an electric field across the material. Many OPVs use bulk heterojunctions (BHJs), meaning that domains of donor and acceptor materials are mixed throughout the material. An alternative to BHJ OPVs is a bi-layer arrangement, where donor and acceptor are in separate films and sandwiched between electrodes.

1.2.2 Charge Carrier Mobility

Charge carrier mobility (CCM) is a measure of how easily charge carriers (electrons and holes, in the case of solids) can move through a material. Charge carrier mobility μ is the relationship between the average drift velocity v_d of charge carriers and the electric field E applied to the material, expressed simply as

$$\mu = \frac{v_d}{E} \tag{2}$$

The value μ is typically expressed in units of $cm^2/V{\cdot}s$. Organic semiconductors typically have mobilities 0.1 $cm^2/V{\cdot}s$, but mobilities as high as 40 $cm^2/V{\cdot}s$ have been observed [14]. For comparison, inorganic semiconductors tend to have mobilities between 100 and 10^4 $cm^2/V{\cdot}s$ [1]. Preliminary work done by Brian Johnson under Oksana Ostroverkhova revealed charge carrier mobilities of up to 0.18 $cm^2/V{\cdot}s$ in xylindein films.

CCM can be calculated for thin films on coplanar electrodes using the following formula:

$$j = \frac{2\mu\epsilon\epsilon_0}{\pi}\frac{V^2}{L^2} \tag{3}$$

where j is current density (or I/d, as will be used later), ϵ is relative permeability, ϵ_0 is permeability of free space, L is distance between electrodes, and V is applied voltage. This equation is applicable in the space charge limited current (SCLC) regime, a region of non-ohmic response where $I \propto V^2$. This regime begins at high applied electric fields (experimentally observed to be around 4×10^3 V/cm for xylindein).

2 Methods

To characterize the properties of xylindein relevant to its potential use as an organic semiconductor, the following measurements were taken: absorption and emission spectra of xylindein solutions (in a range of solvents and under different physical conditions, including adjusted pH and elevated temperatures) and thin films, and current response curves of films to applied voltages. Computational work was also done to calculate the electronic energy levels of xylindein and possible naturally-occurring isomers. All material used in this investigation was extracted directly from fungal culture by the research team of Dr. Sara Robinson (Oregon State University, Department of Forestry).

2.1 Preparation and Characterization of Solutions

Most xylindein solutions tested were prepared by direct mixing of xylindein powder with solvents or by dilution of preexisting solutions (either stock solutions made in-house or HPLC-processed solutions of unknown concentration provided by Sara Robinson). The only exception to this was the solutions used for pH-dependence measurements. These solutions were samples taken from raw fungal culture.

2.1.1 Absorption & Emission Spectra

A typical first step in the optoelectronic characterization of a single molecule is the collection of absorption and emission/photoluminescence (PL) spectra for solutions with very low concentrations. In this case,

solutions with concentrations on the order of 10 μM were used. A solution with this concentration has an average intermolecular separation around 50 nm (see Appendix), while the size of xylindein is on the order of 2 nm, suggesting that there should be minimal interaction between xylindein molecules at this concentration.

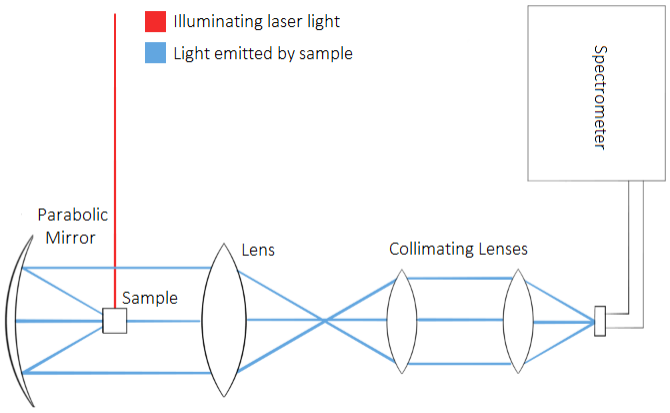

Figure 2: PL measurement setup

The PL spectrum of a sample is the intensity of light at each wavelength emitted by that sample when it is illuminated at a fixed wavelength. In this project, PL spectra were taken by illuminating samples with lasers at 355 nm, 532 nm, and 655 nm and collecting the emitted light with a parabolic mirror directed through lenses and into a fiber optic cable, where it was sent to an OceanOptics spectrometer that collected intensity data (measured as photon counts at a specific wavelength over a specified time interval) and sent it to a computer. This setup is shown in Figure 2. The spectrometer used detects light reliably in the 400-1000 nm range.

An absorption spectrum is a measure of how well a sample absorbs certain wavelengths of light. To collect absorption spectra, light from a tungsten halogen lamp was channeled through a fiber optic cable and directed into sample mount (for solutions, a mount capable of holding a 1 cm wide cuvette, and for films, a bracket mount that allowed light to be shined on the film from the top). Light passing through the sample was collected by another fiber optic cable and processed by an OceanOptics spectrometer. Absorption spectra were calculated using SpectraSuite software by taking an intensity spectrum of the lamp light passed through a sample of pure solvent as a baseline signal and comparing it against the spectrum collected from the xylindein solution. A schematic of the absorption setup is shown in Figure 3.

2.1.2 Temperature Dependence of Spectra

To determine how temperature affects xylindein's optoelectronic properties in solution, absorption was measured for xylindein in chlorobenzene (10 mM concentration) over a range of elevated temperatures ranging from room temperature (20° C) to 200° C. The standard setup for taking absorption measurements was used, except that the mounting assembly and cuvette were attached to a hot plate using thermal grease.

2.1.3 Molar Absorptivity

To calculate molar absorptivity, absorption was measured for solutions of xylindein in chlorobenzene varying in concentration between 6 and 60 μM. These solutions were prepared by taking a 2 mL sample of pure solvent and adding a few microliters of 5 mM xylindein stock solution to it to increase the concentration by a fixed amount.

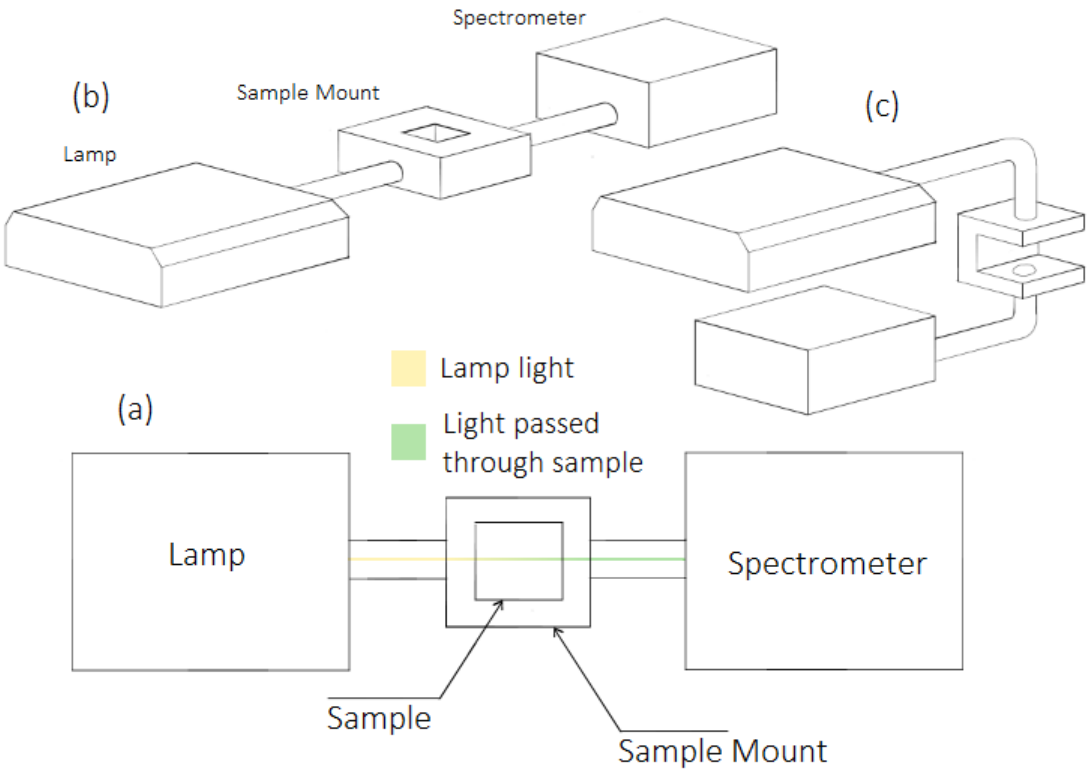

Figure 3: Absorption measurement setup – (a) schematic diagram, (b) solution setup, (c) film setup

To find molar absorptivity, the absorbance of each solution at 655 nm (the dominant peak of xylindein in chlorobenzene) was measured, and absorbance was plotted against concentration. In principle, only one data point would be needed to calculate molar absorptivity. Multiple points were taken at closely-spaced concentrations 1) to confirm that, as expected, absorbance is proportional to concentration in the 1-100 μM range and 2) to average out experimental error.

2.1.4 Photostability

Photostability, as measured by the longevity of a molecule under exposure to visible light, was assessed by putting a xylindein solution under visible light (in this case, the light of a fume hood) and taking absorption measurements weekly. As stated in the above section, the absorptivity of a sample is proportional to its concentration, so the proportion of xylindein remaining can be assessed by comparing the heights and widths of measured absorption peaks against the peaks on the original spectrum. Measurements were taken until the sample was decayed (i.e. none of the characteristic absorption peaks were observed).

The above process was carried out simultaneously for xylindein, ADT-TES-F, and Pn-TIPS. The latter two molecules are benchmark organic semiconductors.

2.2 Characterization of Solvent Effects

2.2.1 Polar vs. Nonpolar

To determine whether or not solvent polarity affects xylindein's behavior in solution, absorption and PL were measured for xylindein in polar and nonpolar solvents. The polar solvents used were isopropyl alcohol (IPA), acetone, and tetrahydrofuran. The nonpolar solvents studied were chlorobenzene, chloroform, and dichloromethane (DCM).

The xylindein solutions in nonpolar solvents were prepared from stock solutions of known concentration. However, since xylindein dissolves poorly in polar solvents, no concentrated stock solutions could be prepared. In addition, because the supply of xylindein powder was limited, only a small amount of xylindein could be used in the preparation of polar solutions. The analytical balance used in the preparation of solutions could only measure masses greater than 0.2 mg, and the amount of xylindein powder used in the creation of the polar solutions was smaller than this. Therefore, only an upper limit on the concentration of these solutions could be calculated.

2.2.2 Protic vs. Aprotic

In addition to studying the effects of solvent polarity, the effect of protic and aprotic solvents was also studied. (These are solvents that do and do not engage in hydrogen bonding, respectively). The protic solvents studied were isopropyl alcohol (IPA) and water (though data from the aqueous xylindein solution is suspect, since the aqueous solution was a sample from a raw fungal culture that likely represented a complex chemical environment). The aprotic solvents used were acetone and tetrahydrofuran (THF).

As in the case of polar and nonpolar solvents, only the effects of proticity on absorption and PL were measured.

2.2.3 pH Effects on Raw Fungal Culture

The effect of solution pH on xylindein was explored using samples of the fungal culture from which xylindein is derived. In particular, the effect of making the solution more basic was investigated by adding small amounts of concentrated NaOH solution to 2 mL samples of unfiltered culture to create solutions with pHs 7, 10, and 13. (The fungal solution itself was slightly acidic, pH 5).

Once absorption and PL measurements had been performed on these solutions, the pH 10 and 13 solutions were brought down to pH 7 by adding concentrated hydrochloric acid to neutralize the NaOH. Characterization of the pH reversed solutions was then performed to test whether or not changes observed in the xylindein spectra were reversible, suggesting that the changes were purely physical, or whether they were irreversible, suggesting that some chemical change had taken place.

2.3 Preparation of Thin Films

In addition to investigating xylindein as a single molecule in solution, the properties of xylindein in the solid state were also explored. There were two main methods used for producing xylindein films: spin casting and drop casting.

2.3.1 Spin Casting

Spin casting is a method of producing a thin film by depositing a small amount of concentrated solution (e.g. 5 μL of 5 mM solution) onto a substrate (in this study, thin glass slides) as the substrate is spun at high speeds (100-3600 rpm) and for up to several minutes. The equipment used for spin casting here worked by creating a vacuum that held the slide to the rotating shaft.

The spin casting process produces films that are highly uniform and very thin, with thicknesses less than a micrometer.

2.3.2 Drop Casting

Drop casting is similar to spin casting, but, rather than relying on centrifugal forces to distribute the material across the substrate, the solution is simply deposited onto a stationary substrate, typically at an elevated temperature.

In contrast to spin casting, drop casting results in films with smaller diameters and greater thicknesses (on the order of 10 μm, see Appendix). However, these films are rarely uniform, and the nature of the solution's solvent and the substrate temperature play a role in the gross morphology of the film.

Because the electrodes used to characterize xylindein's electronic properties were too small to fit on the spin caster mount, all electrode films were produced by drop casting.

2.4 Optimization of Thin Films

To exploit xylindein as a solid state material, methods for creating high-quality (i.e. more crystalline and homogeneous) thin films must be developed. In this study, we explored the optimization of xylindein films.

2.4.1 Background – Determining Film Quality

In the context of optoelectronics, one of the most important features of xylindein as an organic semiconductor is its charge carrier mobility. This metric is the key measure of film quality and can be calculated by taking an IV curve on a xylindein film on an electrode. This procedure, and the method for calculating charge carrier mobility, are discussed in 2.5.2.

2.4.2 Evaporation Times

A key factor affecting crystal growth in concentrated solutions is the rate at which solvent evaporates. Rapid evaporation leads to the growth of small crystals (or, in the case of xylindein, an amorphous structure), which slower evaporation allows crystals to form more slowly and attain larger sizes.

On this basis, one area of testing in film optimization was the characterization of how evaporation time affects film quality. The rate of evaporation in drop-cast solution samples was difficult to control since, as stated above, the volume of solution used to make each film was on the order of microliters. Because these volumes were so small, evaporation rates were not only dependent on solvent and substrate temperature, but on drop topology. In spite of this, drop casting was attempted with an assortment of solvents (including chlorobenzene, dichloromethane, and chloroform) and at a wide range of temperatures (from 7 to 100° C). Observed evaporation times varied from under a second to several minutes.

2.4.3 Solvent Vapor Annealing

Solvent vapor annealing is an annealing method that has yielded excellent results with a wide range of organic thin films. [9, 10] To carry SVA, a slide with a thin film is placed in a closed container (e.g. a closed petri dish) holding a certain amount of solvent. Small amounts of vapor condensing on the film promote continuous, small-scale reorganization. This process can be assisted by creating a temperature differential between the solvent and the film to promote greater condensation, either by heating the solvent reservoir or cooling the film.

Before testing the effect of SVA on xylindein CCM, some pretesting was done using different solvents (chloroform, chlorobenzene, and acetone) on xylindein films on glass slides. Films underwent SVA for 10-15 minutes and were checked under a microscope for any changes in gross morphology, though no changes were observed. SVA using chlorobenzene was carried out on a set of five xylindein films on interdigitated gold electrodes, with five other films used as a control. Initial current-voltage curves were measured for all ten films. Five randomly selected films were then placed on an elevated stage for 20 minutes in a closed petri dish filled partway with chlorobenzene heated to 60° C. New current-voltage curves were then taken on every sample, and the average change in film performance was compared.

2.5 Characterization of Thin Films

2.5.1 Absorption & Emission Spectra

Characterization of the absorption and emission spectra of xylindein films followed the same general process as solution characterization. The only difference was in the mounting hardware. However, since emission from xylindein films is much weaker than it is from solutions, higher exposure times were used in PL measurements.

2.5.2 Current/Voltage Curves and CCM

Since xylindein may have applications as an organic semiconductor, one of its most important features is its response to applied voltages. In order to measure this, xylindein films were drop cast onto gold-film electrodes on a glass substrate. (Aluminum electrodes were also used early on, but these proved to be ineffective). Both sides of an individual electrode pair were connected to a Keithley source measure unit (SMU) via a mount, and voltages ranging from 0 to 300 V were applied. During these sweeps, data on the current flowing through the films was collected, giving IV curves from which charge carrier mobility can be calculated.

Two kinds of gold-film electrodes were used: interdigitated electrodes (where the gap between electrodes takes on a periodic, rectangular pattern, producing electrode "fingers") and coplanar electrodes (where the electrodes are separated by a single, straight gap). While measurements were taken on both, charge carrier mobility can be easily calculated using data from coplanar electrodes. However, treating each finger pair on an interdigitated electrode as an individual coplanar electrode pair allows reasonable estimates to be made using interdigitated electrodes. Each interdigitated electrode used had ten fingers on each electrode, meaning an interdigitated electrode pair is effectively 19 coplanar electrode pairs. Since the length of the fingers and the size of the gaps between them are comparable to the dimensions of the coplanar electrodes used, the assumption that an interdigitated electrode pair will behave like 20 coplanar pairs in parallel will be used.

By using the formula in 1.2.1 relating charge carrier mobility, current, and applied voltage, the CCM of a sample can be calculated by measuring the slope of a plot of current against voltage squared in the SCLC region (assessed by finding the region on the log-log IV plot where the slope jumps from one to two).

$$j = \frac{2\mu\epsilon\epsilon_0}{\pi}\frac{V^2}{L^2} = \frac{I}{d} \tag{4}$$

$$\mu = \frac{\pi}{2\epsilon\epsilon_0}\frac{L^2}{d}\frac{I}{V^2} \tag{5}$$

Where $I \propto V^2$, μ is constant with changing voltages. This means that

$$\mu = \frac{\pi}{2\epsilon\epsilon_0}\frac{L^2}{d}\frac{\Delta I}{\Delta V^2} \tag{6}$$

This formula can be used to directly calculate μ using an IV curve in the SCLC regime.

2.5.3 Film Stability

The fact that xylindein is stable in air is well-established. However, another point of interest is whether or not xylindein remains stable at high temperatures. To test this, a xylindein thin film was prepared on a glass slide, and its absorption spectrum was measured as a baseline. The film was then annealed for ten minute intervals at increasing temperatures, from room temperature to 220°C. Absorption spectra were taken after each interval, and film deterioration was considered complete when xylindein's characteristic peaks were no longer visible.

To get a clearer picture of how quickly xylindein films decay at different temperatures, another test was done. Five xylindein films were prepared on glass slides, and each film was held at a different temperature (50, 100, 150, 175, and 200°C). Absorption spectra were taken on each film after five minutes of exposure to elevated temperatures.

2.6 Theoretical Calculation of Energy Levels

2.6.1 Gaussian 09 and Avogadro

To make theoretical calculations of the characteristics of xylindein and its isomers, virtual models were made in Avogadro, an application that allows the construction and rough geometry optimization of molecules. These models were fed into Gaussian 09, a software suite that uses *ab initio* principles to calculate molecular properties. Whenever Gaussian is run, it produces an input file (*.gjf) on starting and an output file (*.out) on completion. Both of these file types can be opened in any standard text editor.

Gaussian input files consist of four major parts: an instruction line, describing what should be calculated (job type) and how (which functional basis set, what analytical method should be used, and what molecular properties are assumed); a title line; a line to specify the charge of the molecule and its multiplicity (i.e. singlet, doublet, triplet, etc.); and a table of atomic coordinates.

2.6.2 HOMO-LUMO Levels

Knowing xylindein's HOMO and LUMO levels (highest occupies and lowest unoccupied molecular orbitals in the molecule's unexcited state) is of great interest in the context of using xylindein as a semiconductor. For these calculations, the B3LYP method and 6-31G(d,p) basis were used. No job type input was needed, since Gaussian calculates energy levels by default. The results were obtained from a table in the Gaussian output file giving the energies of every occupied molecular orbital ("occ. eigenvalues") and every unoccupied one ("virt eigenvalues"). These values needed to be converted from Hartrees to electron-volts.

2.6.3 Excited State Energies – Singlet & Triplet States

The process of calculating the excited state energies is very similar to the process of calculating ground state energies. The only differences were using the CIS method (a method specifically intended for excited states) and specifying the job with the command TD(root=n), which requests the nth excited state. The energies of the molecular orbitals were, as for the HOMO-LUMO gap, read directly off of tables in the output files.

The triplet state has a complication the singlet state does not. Rather than having just one type of orbital, the triplet state has two: alpha (representing an orbital with a single spin-up electron) and beta (representing an orbital with a single spin-down electron).

2.6.4 Isomers/Tautomers of Xylindein

Since xylindein a) may engage in intramolecular hydrogen bonding between its ketone and alcohol groups and b) has alcohol groups that form enols with with their adjacent double-bonded carbons, the possibility of self-isomerization, including tautomerization (conversion of an enol group to a ketone attached to a single-bonded carbon pair), needed to be explored.

The HOMO-LUMO levels for these isomers were calculated the same way they were for ordinary xylindein. In addition, the enthalpies of formation were calculated for standard xylindein and one of its non-tautomeric isomers (specifically, the one labeled "Edge" in Figure 17, section 3.3). This was done by putting the Freq command in the instruction line, which causes Gaussian to calculate the molecule's vibrational frequencies and thermodynamic properties. The B3LYP method and 6-31G(d,p) basis set were used for this. By comparing enthalpies of formation and assuming the transition enthalpy is not especially different from either of them, the likelihood of self-isomerization can be estimated.

3 Results

3.1 Solution Characterization

The absorption spectrum of a dilute solution of xylindein in chlorobenzene is shown in Figure 4. Though xylindein solutions were stimulated with 355 nm, 532 nm, and 655 nm laser light, a meaningful emission signal was not observed at low concentrations, even at very large integration times (on the order of one second). For comparison, at the same laser power under 355 nm stimulation, an ADT-TES-F solution of comparable concentration showed peak photon counts around 4000 at integration times on the order of a millisecond.

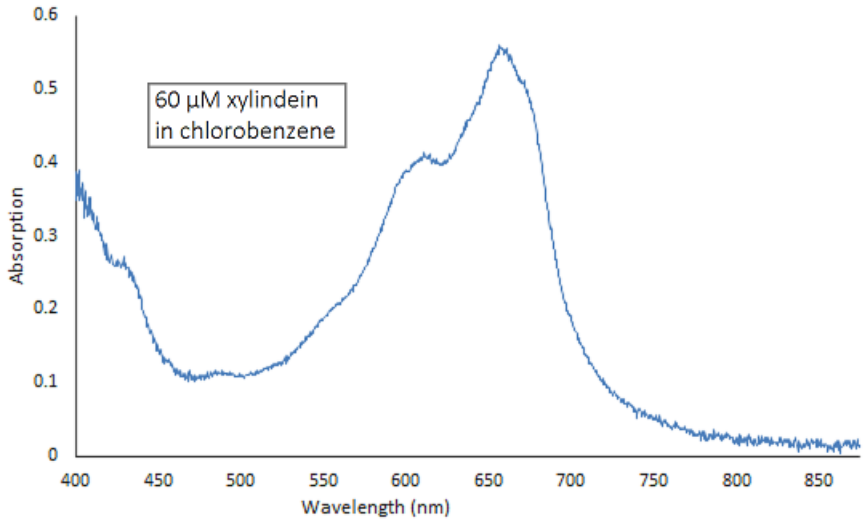

Figure 4: Absorption spectrum of xylindein in chlorobenzene

The photodegradation of a 10 μM solution of xylindein in chlorobenzene and a 10 μM solution of ADT-TES-F in chlorobenzene over thirty weeks is shown in Figure 5. (Data was initially collected for Pn-TIPS as well, but the signal degraded completely in less than a week). Values shown are integrated absorption spectra normalized to the initial value.

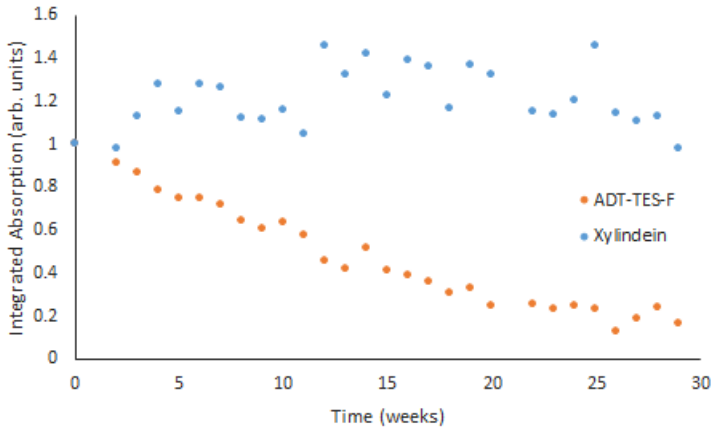

Figure 5: Integrated absorption spectra for xylindein in chlorobenzene (blue) and ADT-TES-F solution (orange) left under exposure to visible light for 30 weeks. Xylindein spectra were integrated from 515 to 800 nm, while ADT-TES-F spectra were integrated from 440 to 550 nm

The adjusted absorption spectra for xylindein in a range of solvents (chlorobenzene, acetone, tetrahydrofuran, isopropyl alcohol, and water) are shown in Figure 6. Because xylindein dissolves poorly in some of these solvents, each spectrum was multiplied by some constant factor to bring all of their peaks to make them all visible and easy to read on the same graph.

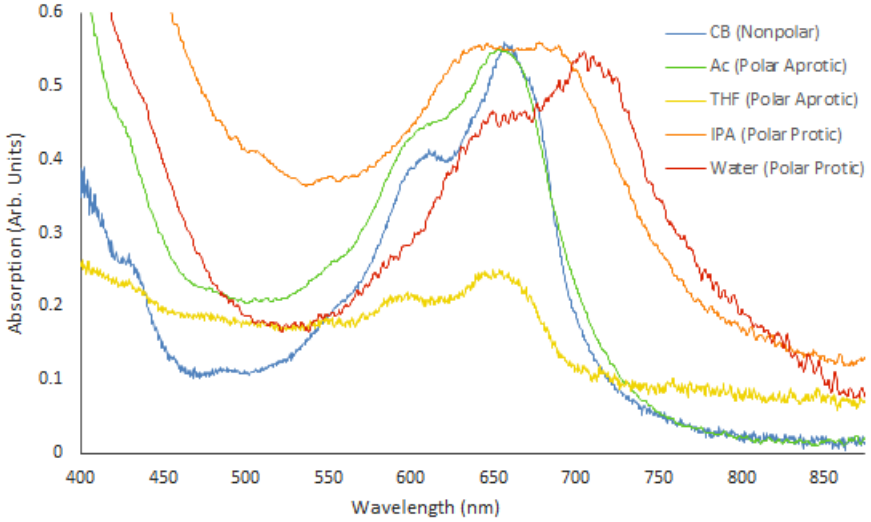

Figure 6: Photostability – Absorption data for xylindein in a variety of polar and non-polar solvents. The peaks in polar and nonpolar aprotic solvents appear to be aligned while a redshift is observed in protic solvents

The response of a solution of xylindein to increased temperatures, as measured by changes in xylindein's absorption spectrum is shown in Figure 7.

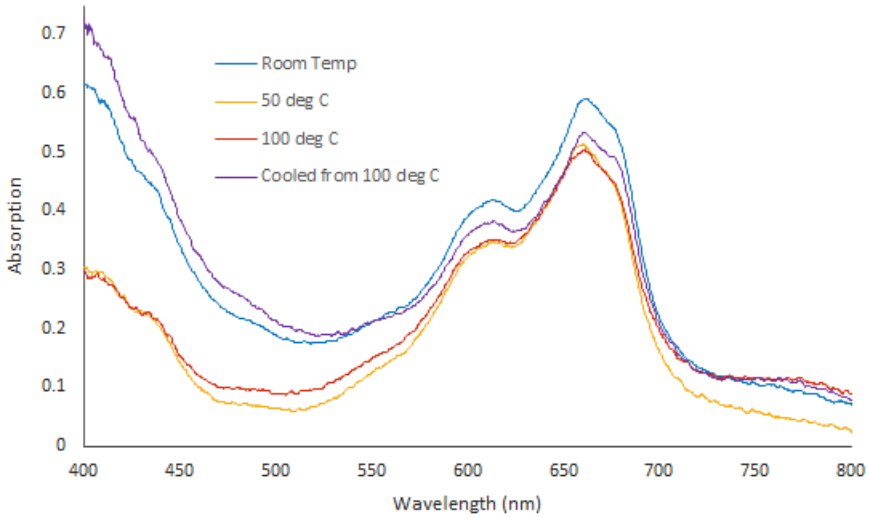

Figure 7: Absorption measurements of a xylindein solution under elevated temperatures

The absorption and PL results (at 355 nm stimulation) for aqueous xylindein from fungal cultures at different pH values are shown in Figures 8 and 9. The sudden drop in the PL reading just before 450 nm is an artifact of a filter used to remove an unwanted signal from the laser. It should be noted that the PL signal observed in Figure 9 comes from a trace impurity in the solution that is observed in both unpurified fungal cultures and solutions prepared from purified xylindein.

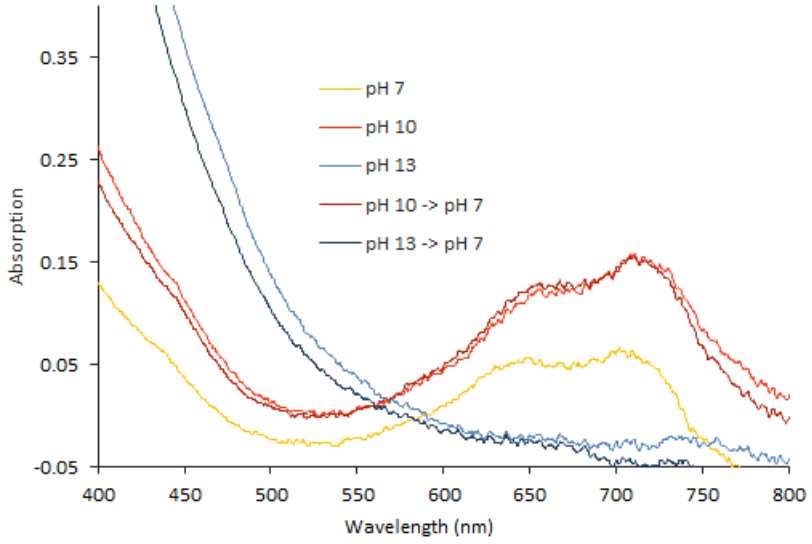

Figure 8: Absorption data for aqueous (water-based) xylindein solutions of various pHs

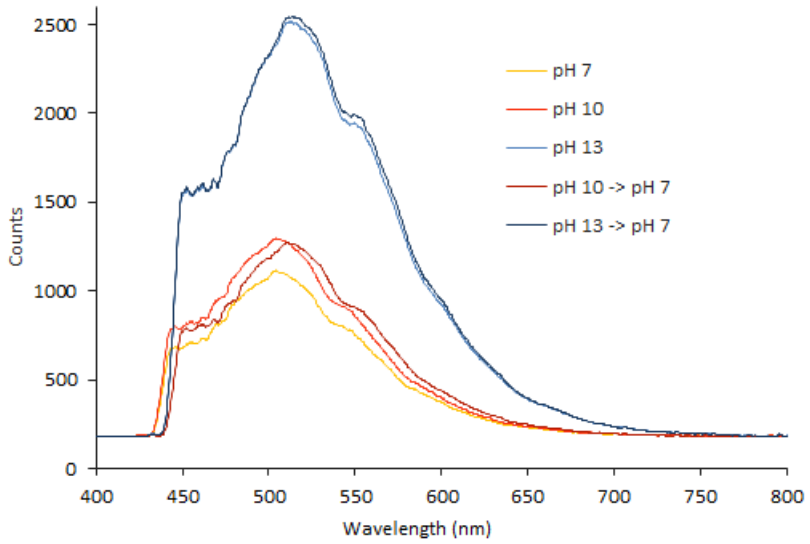

Figure 9: PL data for aqueous xylindein solutions of various pHs

The trend in absorption over small concentrations of xylindein in chlorobenzene, measured by taking the strength of the absorption signal at the 655 nm peak, is shown in Figure 10. A linear fit has been added, since concentration and absorption are directly proportional, as stated in 1.2.4. The slope of this fit line can be used to calculate xylindein's molar absorptivity ϵ, since $\epsilon = \frac{1}{l}\frac{\Delta A}{\Delta c}$. The value of l is 1 cm for the cuvettes used to hold the samples. This means that $\epsilon = 8624\ \frac{1}{\text{M}\cdot\text{cm}}$.

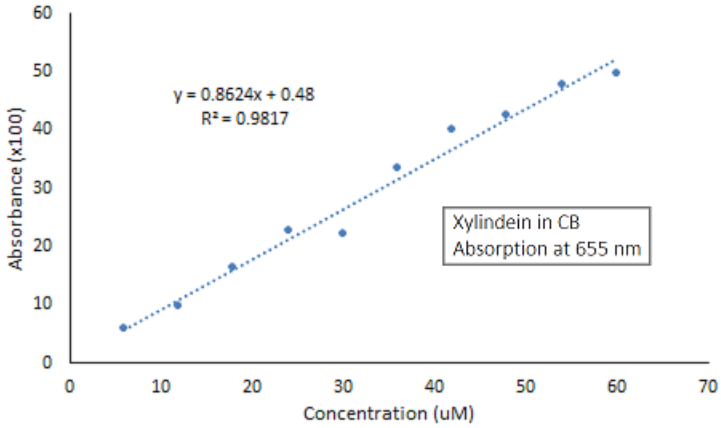

Figure 10: Molar Absorptivity – Absorption of xylindein solutions of varying concentration in chlorobenzene at 655 nm. Molar absorptivity can be calculated from the slope of the best fit line

3.2 Thin Film Characterization

The absorption spectrum for a xylindein thin film is shown in Figure 11. Xylindein films show no appreciable PL, even under very large integration times.

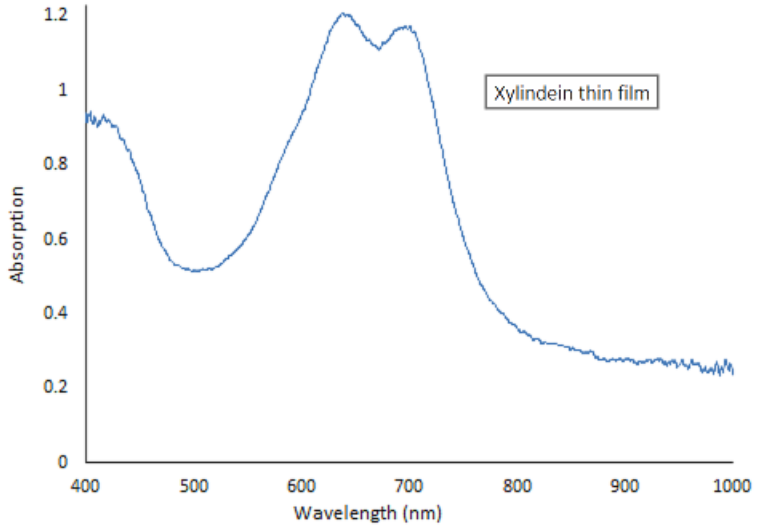

Figure 11: Representative absorption spectrum of xylindein thin films

As a preliminary result, an IV curve taken on a xylindein film on a pair of coplanar gold electrodes, as well as a plot of the slope $n = \frac{\Delta log(I)}{\Delta log(V)}$, is shown in Figure 12. The physical meaning of n is that, assuming I depends on some power of V, $I \propto V^n$. This means that the film is in the SCLC regime when $n = 2$.

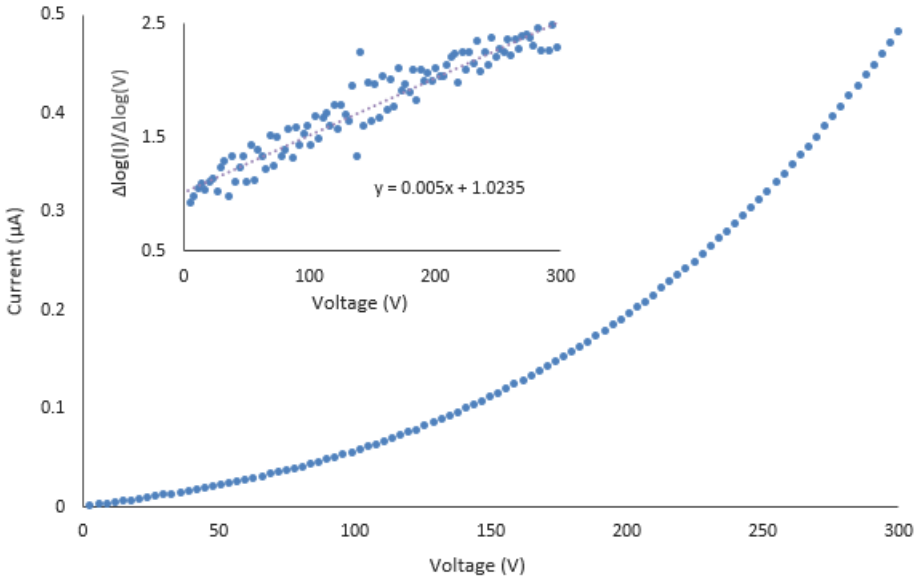

Figure 12: Current-Voltage Curves – Current response in a xylindein film to an applied voltage across a pair of gold, coplanar electrodes. Voltage ranges from 0 to 300 V with steps of 3 V. (*Inset* - Plot of the slopes of the log(I)-log(V) curve)

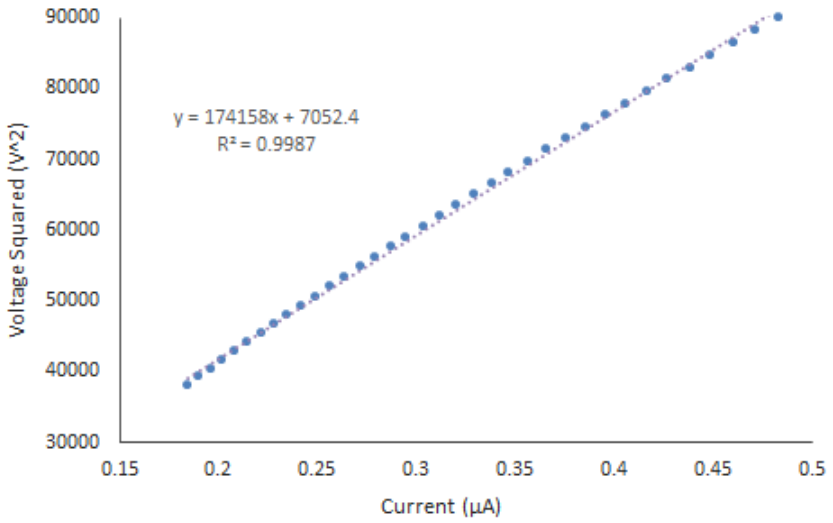

Figure 13: V^2 by I – Voltage squared plotted against current in the SCLC region (i.e. V $\geq$ 195 V) for a xylindein thin film on coplanar electrodes, with linear fit applied

However, because the change from ohmic behavior at low voltages to SCLC behavior gradual, the voltage where the SCLC regime begins is unclear. The value V $\geq$ 195 V was arbitrarily chosen and I was plotted against V^2 for this region, as shown in Figure 13.

Since a linear fit is a good approximation for this data set (with what small curvature there is likely due to fact that n is changing slightly with V), its slope $s = \frac{\Delta V^2}{\Delta I} \approx 1.74 \times 10^{11} \frac{V^2}{A}$ can be used in conjuction with the equation from 2.5.2 to calculate μ:

$$\mu = \frac{\pi}{2\epsilon\epsilon_0} \frac{L^2}{d} \frac{1}{s} \tag{7}$$

Knowing that L = 25 μm, d = 1 mm, and $\epsilon \approx 3$ (within the typical range of permeabilities for organic semiconductors), it can be shown that $\mu \approx 2.21 \times 10^{-3} \frac{\text{cm}^2}{\text{V} \cdot \text{s}}$.

The results of SVA are summarized in Table 1, which shows changes in maximum observed currents for sample and control groups after SVA was carried out, and Figure 14, which shows averaged IV curves pre- and post-SVA for both groups as well as a graph showing plotting maximum currents pre-SVA and post-SVA. The last sample in the control group was excluded from this analysis since it suddenly stopped registering a substantial current.

	SVA					**Control**				
I_{pre}	56	48	30	5	21	69	39 nA	12	36	69
I_{post}	25	18	12	1	2	75	45 nA	13	29	10 nA
$I_{\text{post}}/I_{\text{pre}}$	0.45	0.38	0.40	0.20	0.10	1.09	1.15	1.08	0.80	0

Table 1 - Currents at 300 V for the group that underwent SVA and the control group before (pre) and after (post) SVA was done. Currents are in μ

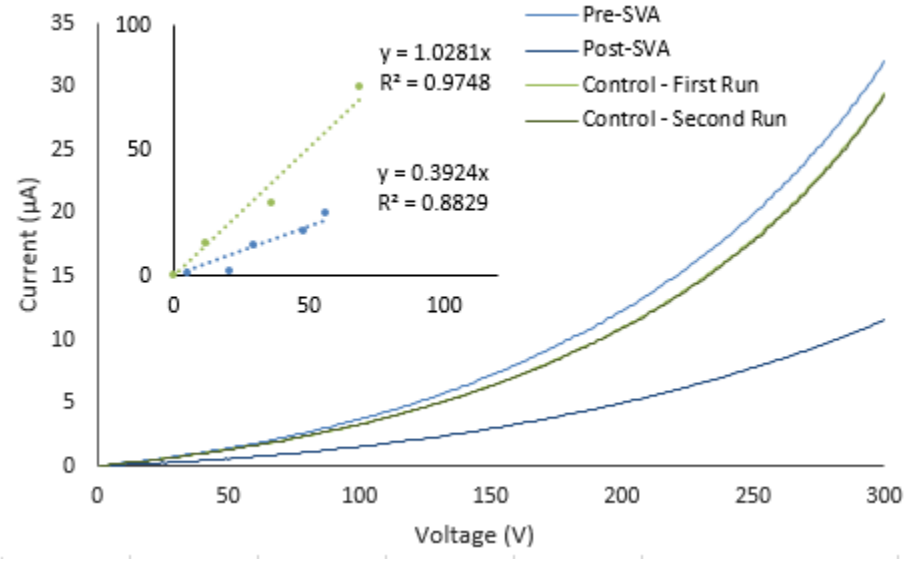

Figure 14: SVA Results – Averaged IV curves for the SVA group (blue) and the control group (green). Darker colors indicate post-SVA results. The curves for the control group overlap almost completely. (*Inset* - Correlation between maximum currents before (x-axis) and after (y-axis) SVA for both groups, with linear fits. Both axes are in μA)

A possible source of unreliability in IV measurements taken on samples on interdigitated electrodes is the fact that, at a fixed applied voltage, current tends to decay, as shown in Figure 15, a graph of the current over time for a sample held at 300 V for 20 minutes. This decay is reversible and is probably not due to xylindein acting as a dielectric. (The amount of charge that would have accumulated on the electrodes if they were acting as a capacitor would have produced a force between them on the order of 10^8 N).

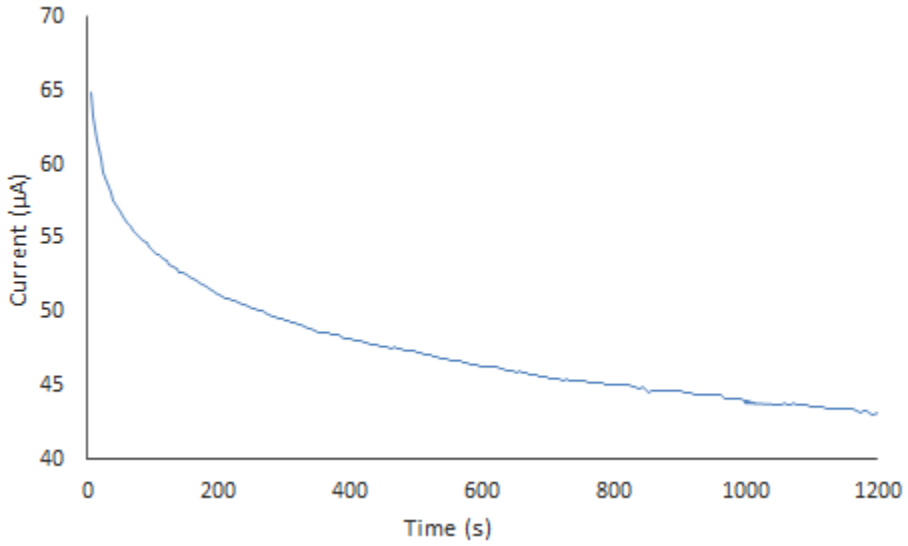

Figure 15: Current decay over time in a xylindein thin film with a voltage of 300 V applied continuously

The absorption spectra taken on a single xylindein film heated to temperatures ranging from room temperature (called 25°C) to 220°C for 15 minutes at a time are shown in Figure 16 (top). The spectra were adjusted for scattering, integrated, and normalized to show relative absorption strength. Figure 17 shows absorption at 640 nm over time for a set of five xylindein films, each held at a different temperature.

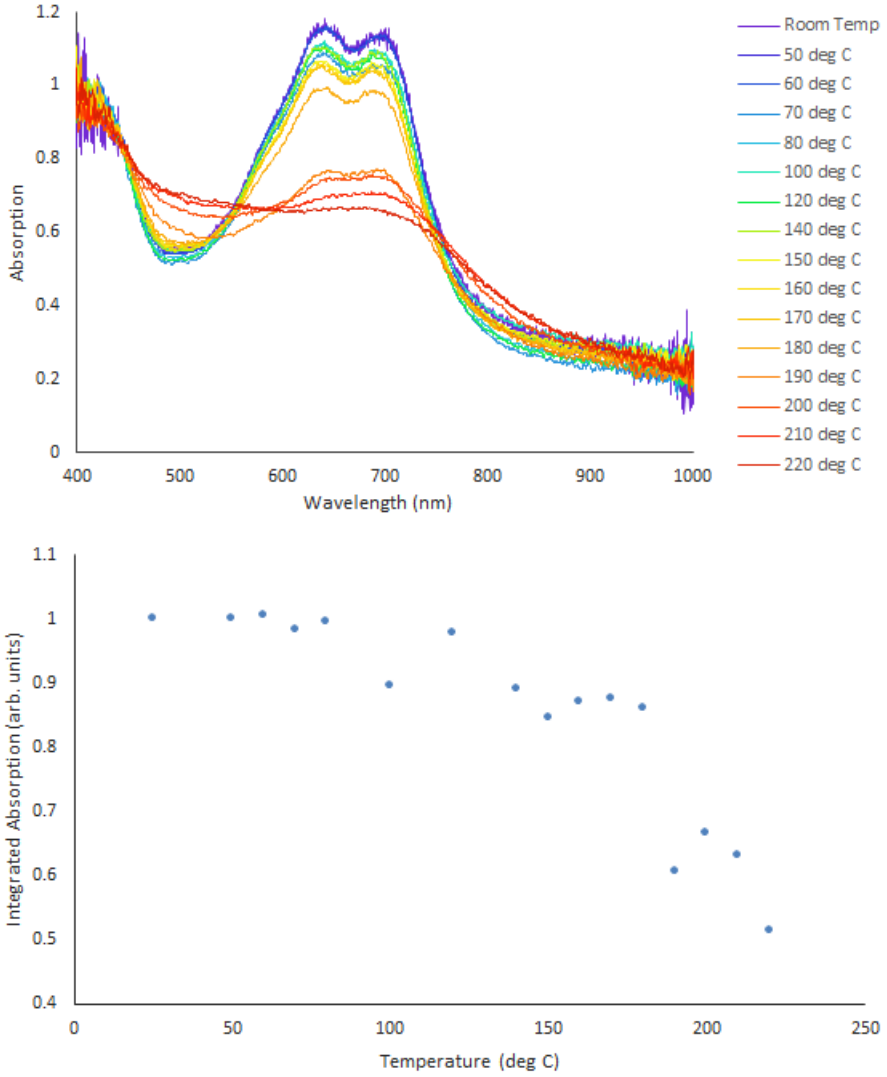

Figure 16: Temperature Stability – Absorption spectra for a xylindein thin film annealed at increasing temperatures, ranging from room temperature (around 25° C) to 220° C (top) – Scattering-adjusted absorption spectra integrated from 475 to 900 nm for each exposure temperature (bottom)

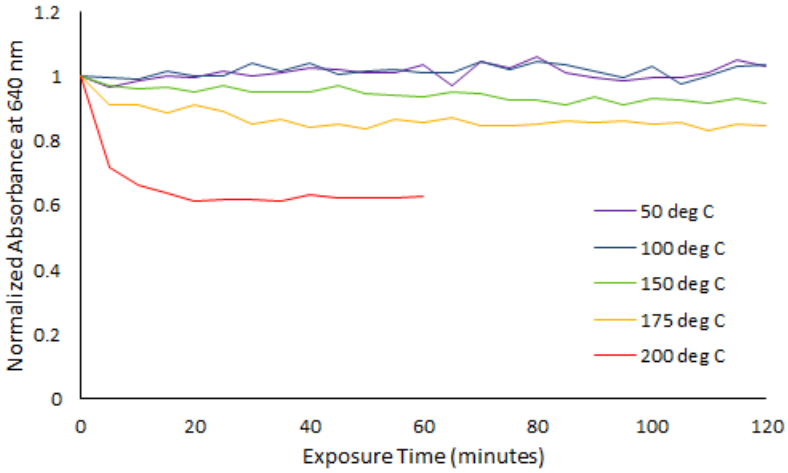

Figure 17: Absorption at 640 nm over time for five xylindein films held at different temperatures

3.3 Theoretical Calculations

The results of the Gaussian 09 calculations are shown in Table 2. Electronic energies have been converted to electron volts (eV) from Hartrees (Ha). Enthalpies of formation have been converted from Hartrees per particle to kilocalories per mole. Photon wavelengths associated with HOMO-LUMO gaps and transitions energies are calculated using the formula $\lambda = \frac{hc}{\Delta E}$. The isomers listed in Table 2 are shown in Figure 18.

Molecule	**HOMO (eV)**	**LUMO (eV)**	ΔE **(eV)**	λ **(nm)**	$\Delta_f H$ **(kcal/mol)**
Xylindein	-6.01	-3.59	2.42	512.3	-1245.98
Edge	-5.70	-3.45	2.24	551.0	-1245.94
Double Edge	-5.84	-3.78	2.06	601.9	N/A
Medial	-5.55	-3.60	1.95	635.8	N/A
Double Medial	-5.49	-3.80	1.70	729.3	N/A
Edge/Medial	-5.50	-3.61	1.89	656.0	N/A

Table 2 - Energy data for xylindein calculated in Gaussian 09

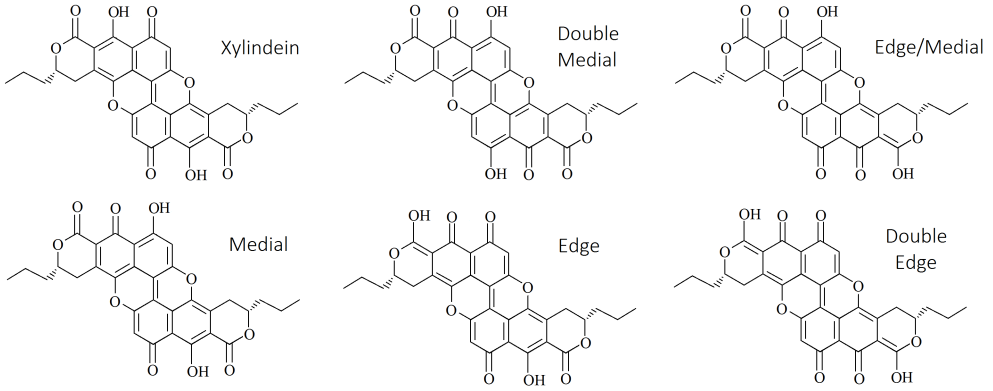

Figure 18: Xylindein and possible isomers formed by internal transfers of hydrogen between oxygens

4 Discussion

From the data laid out above, a few conclusions can be made about xylindein. For one, xylindein is highly stable in an oxygen-rich environment (with stability higher than ADT-TES-F and much higher than Pn-TIPS) up to temperatures above 100°C and under exposure to light.

Comparing the absorption spectra of xylindein in assorted solvents, it is likely xylindein engages in intermolecular hydrogen bonding. The absorption spectra undergo a 30-60 nm redshift in protic solvents (compared to non-polar solvents) that is not observed in polar aprotic solvents. The observed redshift can possibly be explained by coupling between xylindein and solvent molecules and is similar in size to the shift seen in the transition between dilute solutions of xylindein in aprotic solvents and xylindein in the solid state.

In terms of its interactions with light, xylindein has been shown to have a peak molar absorptivity (ϵ =8600 $\frac{1}{\text{M}\cdot\text{cm}}$) similar to other natural pigments. For example, melanin pigments have peak absorptivities in the 1500-82500 range, while chlorophyll mixtures can range from 40000-74400 [11,12]. ADT-TES-F has a peak molar absorptivity around 530 nm that is roughly four times higher than xylindein. However, other viable organic semiconductors often have even higher absorptivities. For example, 3,6-diphenyl-2,5- dihydropyrrolo[3,4-c]pyrrole-1,4-dione (DPP) derivatives can have peak ϵ values in the 10^5 range [13].

Xylindein absorbs light strongly, but it does not emit well, with negligible photon counts from representative solution and film samples even at integration times on the order of seconds. The fact that ADT-TES-F and xylindein fall in the same range with respect to absorptivity but have such radically different PL strengths under the same stimulation suggests that xylindein has very poor quantum yields compared to ADT-TES-F, indicating that xylindein has rapid mechanism(s) (in both dilute and concentrated solutions as well as films) for non-radiative decay.

Efforts to improve xylindein film quality were largely unsuccessful. The average maximum current observed in xylindein films on interdigitated electrodes, about 30 μA, is on the order of magnitide of the results expected from treating each pair of fingers as a coplanar electrode pair with a film similar to the one used for calculating CCM ($0.5\mu\text{A} \times 20 \approx 10\ \mu\text{A}$). SVA seemed to consistently reduce film quality by about 60%, though a larger sample size would be needed to draw firm conclusions. The preliminary CCM of 0.18 $\text{cm}^2/\text{V}\cdot\text{s}$ was not successfully reproduced.

The computational results suggest that 1) the electronic characteristics of xylindein's isomers are highly sensitive to the locations of the hydrogens along the oxygen rows at the edges of the molecule (with HOMO-LUMO gaps ranging from 1.70 to 2.42 eV) and 2) that these isomers have very close enthalpies of formation, indicating that, unless the transition energy is very high, xylindein should isomerize spontaneously. These results are interesting and unexpected, as they predict that multiple absorption spectra should be observed, one for each common isomer. In reality, there appears to be one main spectrum, though a slight "shoulder" does appear on absorption spectra, slightly red-shifted from the main peak. (This shoulder is visible in Figure 4 around 675 nm and is particularly clear in Figure 8).

The results of the investigation into the dependence of aqueous xylindein's optical properties on pH are inconclusive, since the solutions being used were not pure xylindein. However, the absorption and PL data lend themselves to some interpretations. High pH causes xylindein's characteristic absorption peaks to disappear irreversibly, implying that the xylindein is either destroyed or modified. As the expected absorption spectrum disappears, the strength of the PL spectrum in the UV region grows, likely due to products of xylindein decomposition.

5 Conclusion

Though the high CCM observed in early bulk samples was not reproduced successfully, a variety of useful new conclusions can be drawn about xylindein as an organic semiconductor. Xylindein has been shown to have good stability under exposure to light and at high temperatures under normal atmospheric conditions. Xylindein also absorbs light moderately well, though its strong non-radiative decay mechanisms could be problematic for use in certain applications.

Ongoing work is being done on the use of xylindein for device applications, including collection of photocurrent data for both xylindein and xylindein admixtures (e.g. mixtures of xylindein and PMMA, P3HT, etc.) and continued work to improve the quality of xylindein films.

Acknowledgments

This project was possible thanks to my advisor, Dr. Oksana Ostroverkhova, who provided help and guidance at every stage of the project, and Robert Harrison, with whom much of the data presented in this report was taken. Funding for this project was provided in part by the NSF grant NSF-CBET-170599 and the URISC program. Feedback from Dr. Janet Tate and the students of the PH403 class helped in the writing of this report.

References

1. "The path to ubiquitous and low-cost organic electronic appliances on plastic." Forrest, Stephen R. *Nature* **428**, 911-918 (2004).
2. "Biocompatible and Biodegradable Materials for Organic Field-Effect Transistors." Irimia-Vladu, Mihai et al. *Advanced Functional Materials* **20**, 4069-4076 (2010).
3. "Hydrogen-Bonded Semiconducting Pigments for Air-Stable Field-Effect Transistors." Głowacki, Eric Daniel et al. *Advanced Materials* **25**, 1563-1569 (2013).
4. "IndigoA Natural Pigment for High Performance Ambipolar Organic Field Effect Transistors and Circuits." Irimia-Vladu, M. et al. *Advanced Materials* **24**, 375-380 (2012).
5. "25th Anniversary Article: A Decade of Organic/Polymeric Photovoltaic Research." Dou, Letian, et al. *Advanced Materials* **25**, 6642-6671 (2013).
6. "Fullerene-based Schottky-junction organic solar cells: a brief review." Sutty, S., Williams, G. & Aziz, H. *J. Photonics Energy* **4**, 040999 (2014).
7. "Non-Fullerene Organic Solar Cells with 6.1% Efficiency through Fine-Tuning Parameters of the Film-Forming Process." Zhang, Xin, Chuanlanf Zhan, Jiannian Yao. *Chemistry of Materials* **27**, 166-173 (2015).
8. "Stimulating growth and xylindein production of Chlorociboria aeruginascens in agar-based systems." Robinson, S. C., Tudor, D. & Snider, H. *AMB Express* **2**, (2012).
9. "Solvent vapour annealing of organic thin films: controlling the self-assembly of functional systems across multiple length scales." De Luca, Giovanna, et al. *Journal of Materials Chemistry* **20**, 2493-2498 (2010).
10. "Solvent vapor annealing on perylene-based organic solar cells." Grob, Stefan, et al. *Journal of Materials Chemistry A* **3**, 15700-15709 (2015).
11. "Spectrophotometric Analysis of the Mixtures of Photosynthetic Pigments." Gadzaru, D.M., B. Iorga. *Journal of Optoelectronics and Advanced Materials* **4**, 121-129 (2002).
12. "Estimation of molar absorptivities and pigment sizes for eumelanin and pheomelanin using femtosecond transient absorption spectroscopy." Piletic, Ivan R., Thomas E. Matthews, Warren S. Warren. *Journal of Chemical Physics* **139**, (2009).
13. "Development of New Organic Semiconductors and Their Applications in Organic Electronics and Photonics." Weiter, Martin, Martin Vala, Jan Vyňuchal, Lubomír Kubač. *NanoCon* **10**, 12-14 (2010).
14. "Organic Optoelectronic Materials: Mechanisms and Applications." Ostroverkhova, Oksana. *Chemical Reviews* **116**, 13279-13412 (2016).

Appendix

Molecular Spacing in Solution

For a solution with a concentration M, assuming the solute molecules are spaced evenly throughout the solution, the average intermolecular spacing is $l = (\bar{V})^{1/3}$, where $\bar{V}$ is the volume of the solution per molecule of solute. By the definition of molarity M (moles per unit volume), $\bar{V} = (N_A M)^{-1}$, where N_A is Avogadro's number. This means that, for a solution for which $M = 10$ μM (or 10 μmol per liter), the average intermolecular spacing is

$$\begin{aligned} l &= (\bar{V})^{1/3} \\ &= (N_A M)^{-1/3} \\ &= (6.022 \times 10^{23} \frac{1}{1 \text{ mol}} \times 10 \times 10^{-6} \frac{1 \text{ mol}}{1000 \text{ cm}^3})^{-1/3} \\ l &= 55 \text{ nm} \end{aligned}$$

The same calculation can be done for concentrations of 20 and 200 μM, leading to mean intermolecular spacings of 44 and 20 nm respectively.

Drop Cast Film Thickness

The thickness h of a drop cast film can be estimated by measuring the diameter D of the film, calculating the film's mass m, estimating the density ρ of solid xylindein based on the densities of similar organic materials, and assuming that the film is roughly cylindrical, with a volume $V = \frac{\pi h D^2}{4}$. Having an expression for V, the formula $m = V\rho$ can be rearranged to find h,

$$h = \frac{4m}{\pi \rho D^2}$$

Film mass m can be calculated from the volume U and molarity M of the drop casting solution as long as the molar mass X of xylindein, 568.53 g/mol. A typical drop cast xylindein film is produced using 10 μL of 10 mMol solution, meaning that a typical film mass is around

$$\begin{aligned} m &= XMU \\ &= (568.53 \frac{\text{g}}{\text{mol}})(10 \times 10^{-3} \frac{\text{mol}}{\text{L}})(10 \times 10^{-6} \text{ L}) \\ m &= 57 \mu\text{g} \end{aligned}$$

The density of xylindein can be assumed to be on the order of 1 g/cm^3, and a typical film has a diameter of about 3 mm. With these values, film thickness h can be estimated to be

$$\begin{aligned} h &= \frac{4 \times 57 \times 10^{-6} \text{g}}{\pi \times 1 \frac{\text{g}}{\text{cm}^3} \times (0.3 \text{ cm})^2} \\ &= 8.0 \times 10^{-4} \text{ cm} \end{aligned}$$

So the thickness of a drop cast film is on the order of 10 μm.